

Geoscience Laser Altimeter System (GLAS) Final Test Report of DM LHP TV Testing

C. Baker

National Aeronautics and
Space Administration

Goddard Space Flight Center
Greenbelt, Maryland 20771

The NASA STI Program Office ... in Profile

Since its founding, NASA has been dedicated to the advancement of aeronautics and space science. The NASA Scientific and Technical Information (STI) Program Office plays a key part in helping NASA maintain this important role.

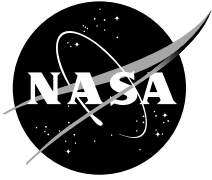
The NASA STI Program Office is operated by Langley Research Center, the lead center for NASA's scientific and technical information. The NASA STI Program Office provides access to the NASA STI Database, the largest collection of aeronautical and space science STI in the world. The Program Office is also NASA's institutional mechanism for disseminating the results of its research and development activities. These results are published by NASA in the NASA STI Report Series, which includes the following report types:

- **TECHNICAL PUBLICATION.** Reports of completed research or a major significant phase of research that present the results of NASA programs and include extensive data or theoretical analysis. Includes compilations of significant scientific and technical data and information deemed to be of continuing reference value. NASA's counterpart of peer-reviewed formal professional papers but has less stringent limitations on manuscript length and extent of graphic presentations.
- **TECHNICAL MEMORANDUM.** Scientific and technical findings that are preliminary or of specialized interest, e.g., quick release reports, working papers, and bibliographies that contain minimal annotation. Does not contain extensive analysis.
- **CONTRACTOR REPORT.** Scientific and technical findings by NASA-sponsored contractors and grantees.
- **CONFERENCE PUBLICATION.** Collected papers from scientific and technical conferences, symposia, seminars, or other meetings sponsored or cosponsored by NASA.
- **SPECIAL PUBLICATION.** Scientific, technical, or historical information from NASA programs, projects, and mission, often concerned with subjects having substantial public interest.
- **TECHNICAL TRANSLATION.** English-language translations of foreign scientific and technical material pertinent to NASA's mission.

Specialized services that complement the STI Program Office's diverse offerings include creating custom thesauri, building customized databases, organizing and publishing research results . . . even providing videos.

For more information about the NASA STI Program Office, see the following:

- Access the NASA STI Program Home Page at <http://www.sti.nasa.gov/STI-homepage.html>
- E-mail your question via the Internet to help@sti.nasa.gov
- Fax your question to the NASA Access Help Desk at (301) 621-0134
- Telephone the NASA Access Help Desk at (301) 621-0390
- Write to:
NASA Access Help Desk
NASA Center for AeroSpace Information
7121 Standard Drive
Hanover, MD 21076-1320



Geoscience Laser Altimeter System (GLAS) Final Test Report of DM LHP TV Testing

Charles Baker, Orbital, Greenbelt, Maryland

National Aeronautics and
Space Administration

Goddard Space Flight Center
Greenbelt, Maryland 20771

Acknowledgments

I would like to personally thank Dan Butler (GSFC), Jentung Ku (GSFC), and Tarik Kaya (ISU) for their tireless hours in conducting this long thermal vacuum test, and then their subsequent technical review and commentary of the data reduction and report. Without these gentlemen, the testing and data reduction could not have been as extensive and conclusive as has been outlined in this report.

The test setup itself was designed and built in half the expected required time thanks to the long hours contributed by Mario Martins (Swales). He was always willing to spend the time to work through bugs until the test could be setup correctly and every Watt understood.

Michael Nikitkin (DCI) and Walter Bienert (DCI) have been my mentors for years. Much of their expertise and problem-solving techniques were employed in my models of this Development Model Loop Heat Pipe. In addition, Michael was personally responsible for the successful manufacture of the Loop Heat Pipe.

Eric Grob (GSFC), as the thermal lead for GLAS, always knew how to ask the right questions. His understanding of the test's importance allowed all of the important questions to be answered.

This is, of course, not to belittle the small army of people required to monitor this test two shifts a day who I didn't thank personally in this section. Lastly, my thanks to the Goddard Space Flight Center's Code 545, The Thermal Branch, for its strong support.

Available from:

NASA Center for AeroSpace Information
7121 Standard Drive
Hanover, MD 21076-1320
Price Code: A17

National Technical Information Service
5285 Port Royal Road
Springfield, VA 22161
Price Code: A10

TABLE OF CONTENTS

1.0 INTRODUCTION	1
2.0 TEST SETUP	1
2.1 Documentation	1
2.2 Flight LHP System	1
2.3 DM LHP System	1
2.4 Test Plan	6
2.5 Thermocouple Diagram	7
3.0 STARTUP TESTS	9
3.1 Effect of Initial Condenser Temperature	11
3.2 Effect of Initial Evaporator Temperature	11
3.3 Effect of Single Laser Mass Simulator Power	11
3.4 Startup Heater Power Sensitivity (0 W, 15 W, 20 W)	11
3.5 Reflux vs. Adverse Effects	13
3.6 Repeatability of Startup Test	13
4.0 CONTROL HEATER POWER TESTS	13
4.1 Control Heater Power Energy Balance	15
4.2 Temperature Stability	15
4.3 Sink Condition Effect	15
4.4 Sensitivity to Setpoint	15
4.5 Sensitivity to a Changing CC Setpoint	17
4.6 Transient Sink Effects (with Fixed Conductance Mode)	18
4.7 Adverse vs Reflux	19
4.8 Number of Block Couplings	19
4.9 Effect vs. Laser Simulator Power	21
5.0 LHP CONDUCTANCE/TRANSPORT	21
5.1 Evaporator Conductance	22
5.2 Condenser Conductance	22
6.0 POWER TRANSIENTS	24
7.0 LOW POWER LONG TERM STEADY STATE TESTS	25
8.0 PREVENTING THE CC FROM FLOODING THE EVAP	27
9.0 CONCLUSIONS	27
10.0 TV TEST RECOMMENDATIONS	27

LIST OF FIGURES

Figure 1. Flight LHP configuration	2
Figure 2. DM LHP Test Setup.	3
Figure 3. Starter heater location.	4
Figure 4. Compensation chamber layout.	4
Figure 5. Liquid - Vapor line coupling blocks.	5
Figure 6. MLI blanketing.	5
Figure 7. Heater Plates.	6
Figure 8. TC diagram.	8
Figure 9. Typical startup.	9
Figure 10. Temperature stability at the laser mass simulator.	17
Figure 11. Control Heater Power vs. Delta T between CC and Condenser Exit.	18
Figure 12. Control Heater Power Transient.	20
Figure 13. LHP DM 205 W temperatures compared to test data.	24
Figure 14. LHP DM 114 W temperatures compared to test data.	24
Figure 15. Low power long term steady state.	25
Figure 16. Increasing setpoint at a rate of 0.6° C/5 minutes.	26

Diagram 1	21
-----------------	----

LIST OF TABLES

Table 1. Setpoints for various.	6
Table 2. Thermal Vacuum Testing.	7
Table 3. DM LHP Startup Matrix.	10
Table 4. Startups vs. Starter Heater Power.	12
Table 5. DM LHP Control Power Test Matrix 2.0	14
Table 6. Calculation of Control Heat Power	16
Table 7. Compare Control Heater Power vs. LHP Orientation	19
Table 8. Individual Test Block Couplings	23
Table 9. Assumptions for DM LHP Evaporator Model	23
Table 10. Condenser Conductance	25

1.0 INTRODUCTION

The Demonstration Model (DM) Loop Heat Pipe (LHP) was tested at Goddard Space Flight Center (GSFC) during September and October, 1999. The LHP system was placed in the Dynavac 36" chamber in Building 4. The test lasted for about 6 weeks. The LHP was built, designed, and manufactured at Dynatherm Corporation, Inc. in Hunt Valley, MD according to GSFC specifications. The purpose of the test was to evaluate the performance of a propylene LHP for the Geoscience Laser Altimetry System (GLAS) instrument application.

2.0 TEST SETUP

2.1 Documentation

GLAS-545-SPEC-005
GE-2025935
GE-2025969

Test Plan for Geoscience Laser Altimeter System
Loop Heat Pipe Laser Thermal System Development Unit
Test Assembly, LHP System, Laser Development Unit

2.2 Flight LHP System

The Geoscience Laser Altimetry System (GLAS) Development LHP Test was designed to resemble the flight laser LHP. The flight system has three lasers attached to three heat pipes which run to the LHP evaporator, see Figure 1. The heat is dissipated in one of the lasers and conducted through one of the heat pipes to the LHP evaporator. The LHP evaporator is then coupled to a radiator panel, which radiates the heat to space. LHPs can operate in fixed and variable conductance modes. This allows the setpoint of the LHP evaporator to be maintained at a steady temperature and meet the tight stability requirements of the internal components.

The radiator panel is designed to actively radiate from both sides of the radiator panel. On the LHP side of the radiator panel, most of the radiator views the interior of the instrument, however the upper portion is exposed to the space environment. The other radiating surface encompasses the entire planar area of the radiator panel. In the flight case, these radiating surfaces are covered with 6 mil OSRs.

2.3 DM LHP System

For DM LHP, the radiator surfaces were covered in 3 mil VDA-backed Kapton which has a similar emissivity to OSRs. The LHP evaporator was reoriented near the radiator panel to fit into the thermal vacuum chamber, see Figure 2. Two mass simulators were used to represent the three lasers. DM LHP used all of the thermal mass of the flight lasers, but lumped the two inactive lasers into one mass simulator that has twice the thermal mass of one flight laser. In the flight case and in the DM LHP setup, the lasers (or mass simulators) and the LHP are radiatively and conductively isolated from the surrounding structure except through the conducting HPs. For the DM LHP, a test stand was designed similar to Figure 2 which mechanically supported the LHP Radiator panel, and two mass simulators, while thermally isolating them. During testing, the test stand was heated to near the system temperature to eliminate parasitics between the LHP system and the test stand.

The flanged heat pipes were bolted to the mass simulator along a 14" flange. Apeizon L thermal grease was used as the interface material. Bondline was ~.001". The heat pipes were machined round and fit into a clamshell-type joint between the LHP evaporator and an adjoining clamp. The joints were machined to have little or no bondline thickness and Apeizon L thermal grease was used as the interface material. The evaporator was 12" long with bolt spacing every 1.1" and Apeizon L thermal grease was used as the interface material.

G10 spacers were used to isolate the LHP evaporator and mass simulators from the test stand. The radiator panel was also isolated from the test stand with G10 spacers.

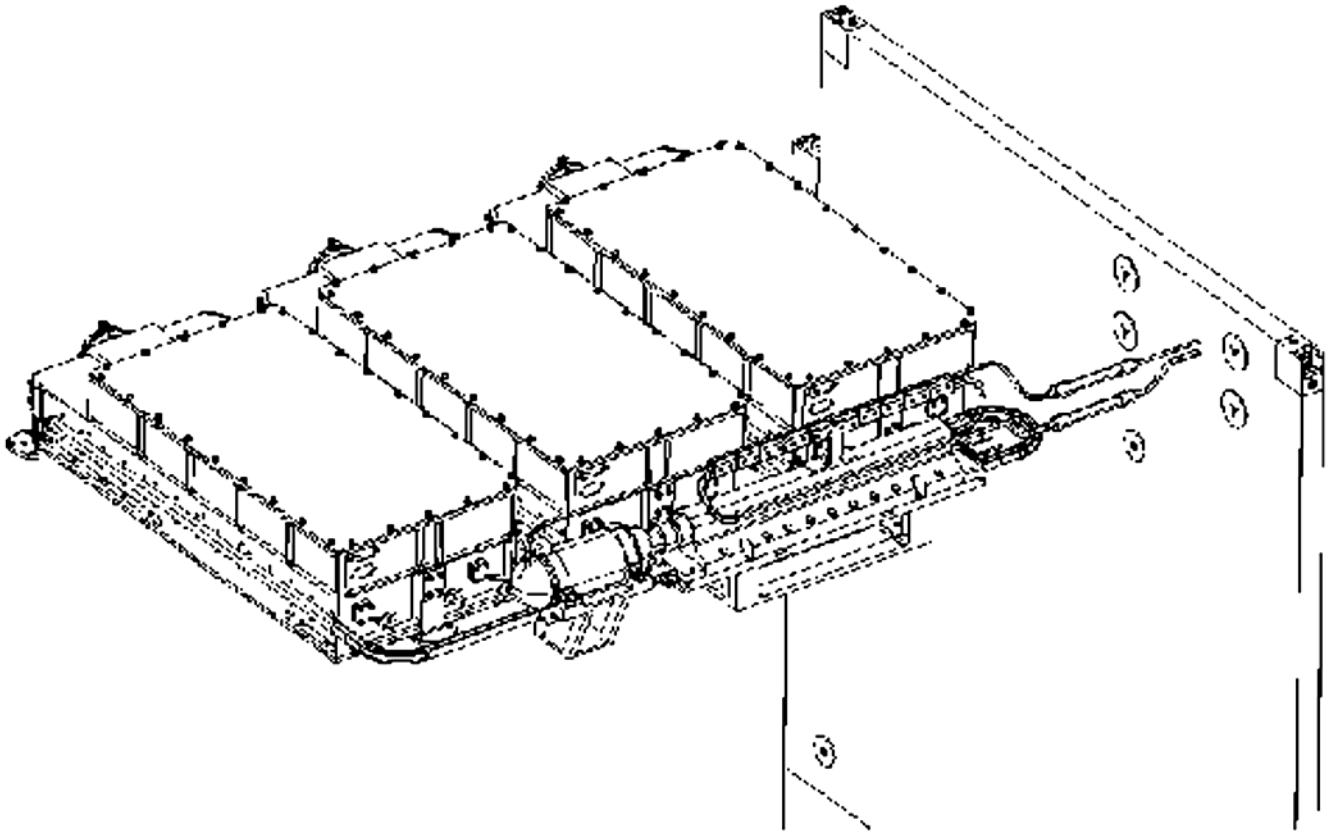


Figure 1. Flight LHP configuration.

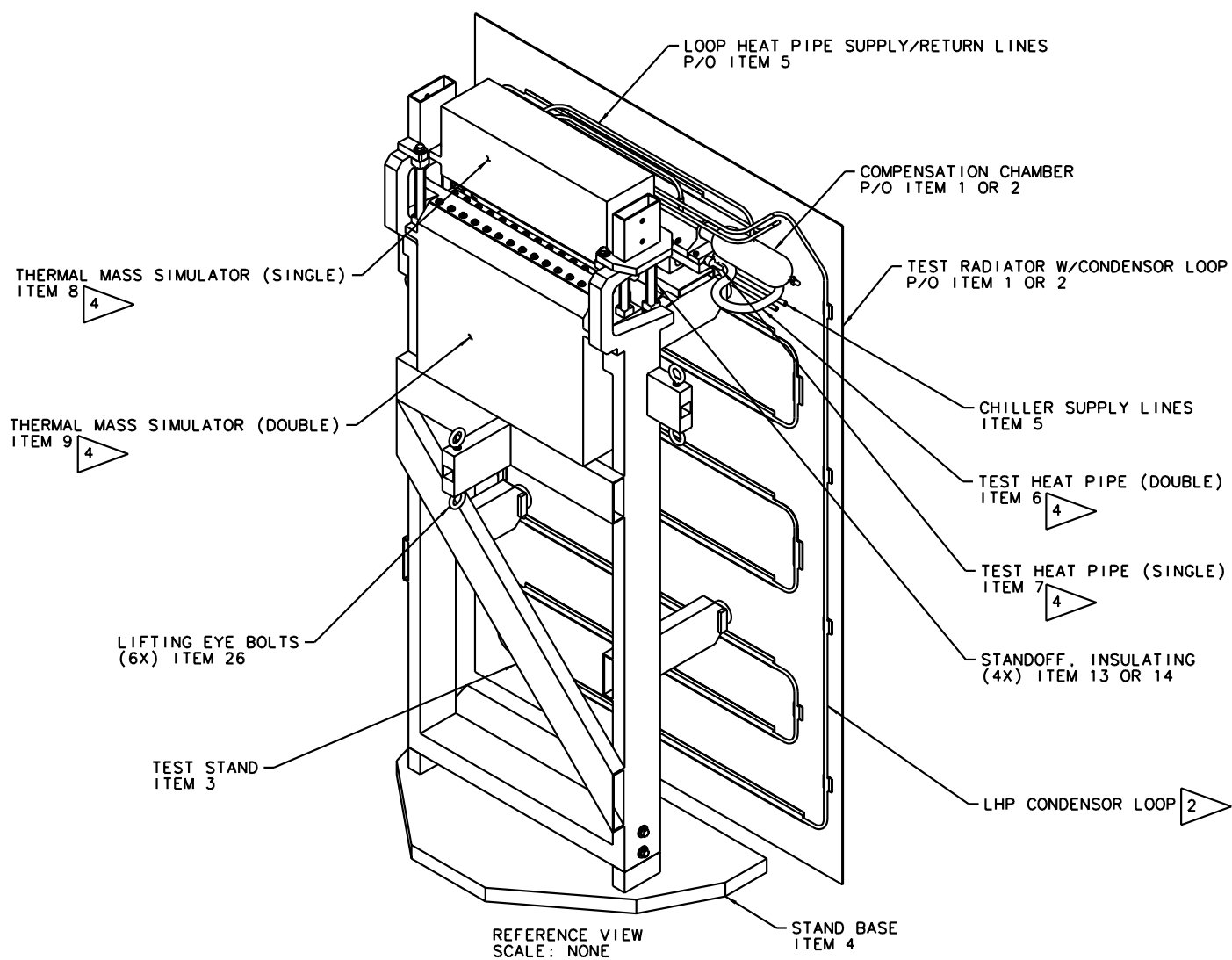


Figure 2. DM LHP Test Setup.

Cartridge heaters were placed within the mass simulators to represent the heat dissipation of the lasers. A Dale NHG-25 50 Ohm resistor with a footprint 0.56" x 1.1" starter heater was placed 1" from the end of the LHP to assist with startup. This starter heater was attached to the LHP evaporator with ~0.005" thick Stycast 2850 FT epoxy and secured with a stainless steel strap. The location of the starter heater is shown in Figure 3.

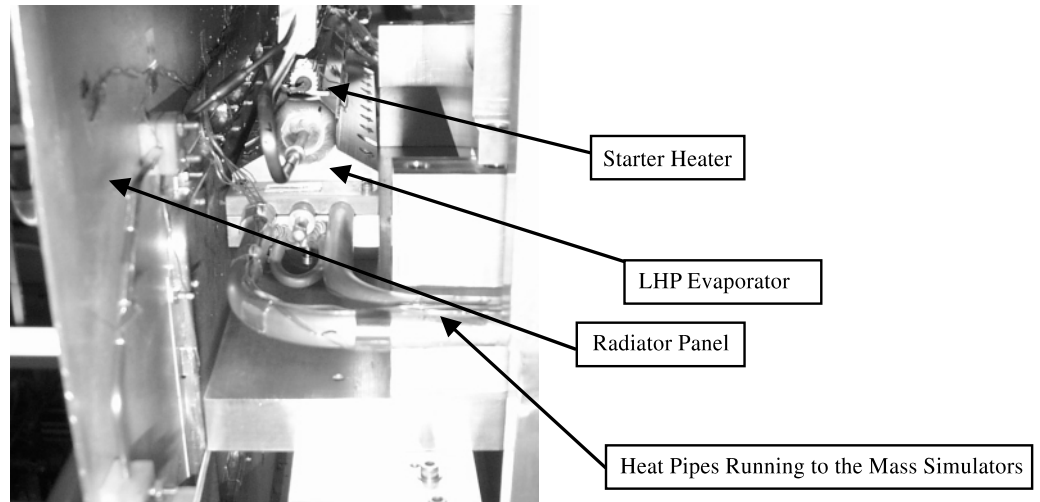


Figure 3. Starter heater location.

The radiator panel was always oriented in the vertical plane during all testing. The control sensor for the LHP Compensation chamber (CC) was located near the middle of the CC. The control heater was wrapped circumferentially and overtaped with aluminum tape. Figure 4 shows the compensation chamber from the side. The orientation of this photo is similar to Figure 2.

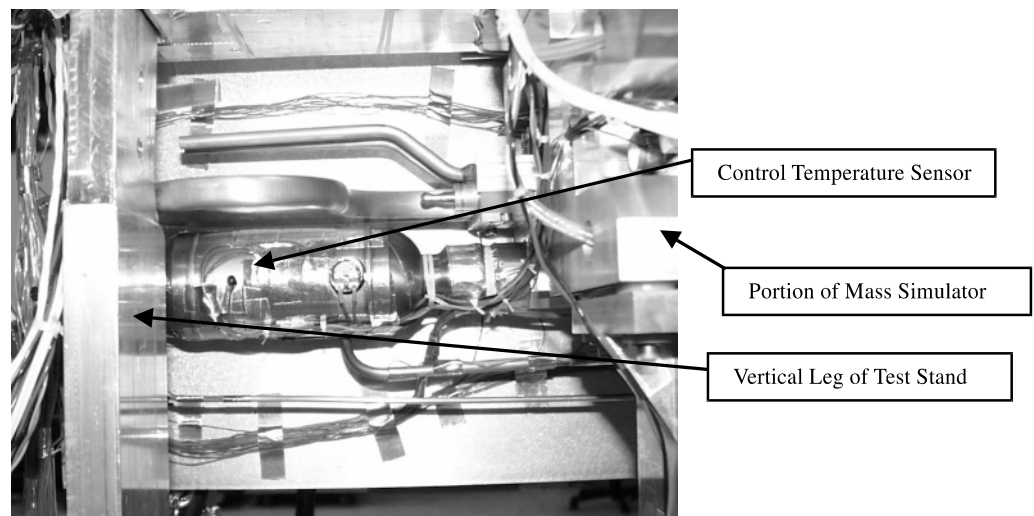


Figure 4. Compensation chamber layout.

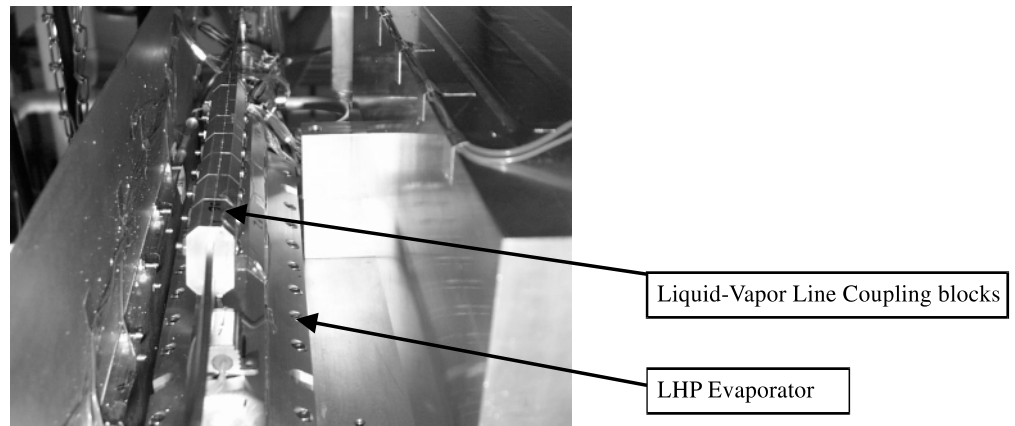


Figure 5. Liquid - Vapor line coupling blocks.

Aluminum coupling blocks were added between the liquid and vapor lines. These coupling blocks reduced the liquid temperature entering the compensation chamber and thus minimized the control heater power. These coupling blocks were clamped to the liquid and vapor lines with NuSil CV-2948 as an interface material. The blocks are shown in Figure 5 running above the LHP evaporator and starter heater.

All thermally coupled components were externally MLI blanketed to thermally decouple them from the environment and from each other. Care was taken to blanket the mass simulators, heat pipes, LHP evaporator and transport lines, portions of the test stand, and inactive portions of the radiator. Figure 6 shows the blanketing surrounding the mass simulators and backside of radiator panel. In this Figure the LHP evaporator is shown at the bottom near the base of the Test stand, opposite to Figure 2. This orientation is the reflux orientation (condenser panel mainly above LHP evaporator.) Figure 2 shows the adverse orientation (LHP evaporator above the condenser panel.) Note that the radiator panel is always vertical.

The environmental loading of the radiator panel was simulated during this test by heater plates. Separate heater plates faced both sections of the radiator. The heater plates were temperature controlled to a setpoint and the shroud was temperature controlled to another setpoint. The heater plates were suspended from the test stand but isolated. The heater plates were about 6" from the radiator on both sides. Figure 7 shows the heater plates attached to the test stand. The LHP is shown in reflux mode.

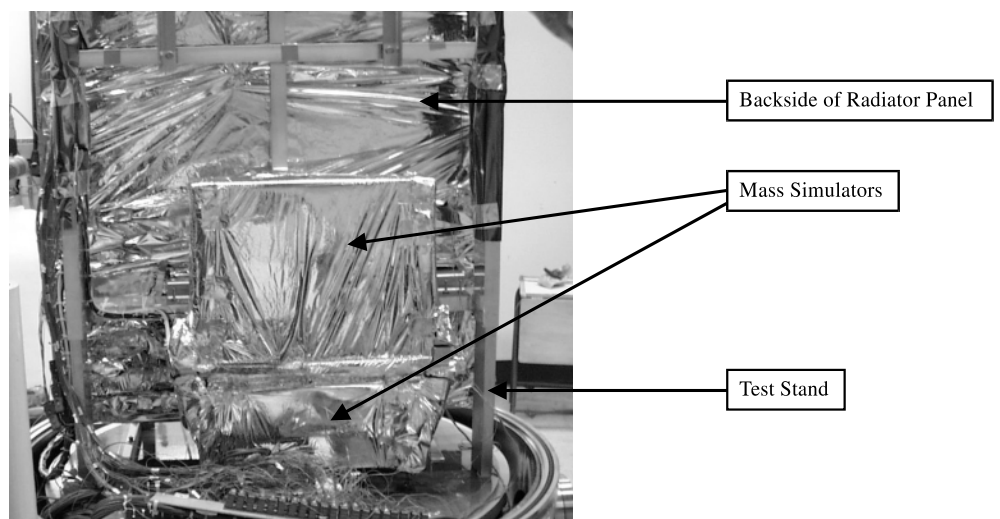


Figure 6. MLI blanketing.

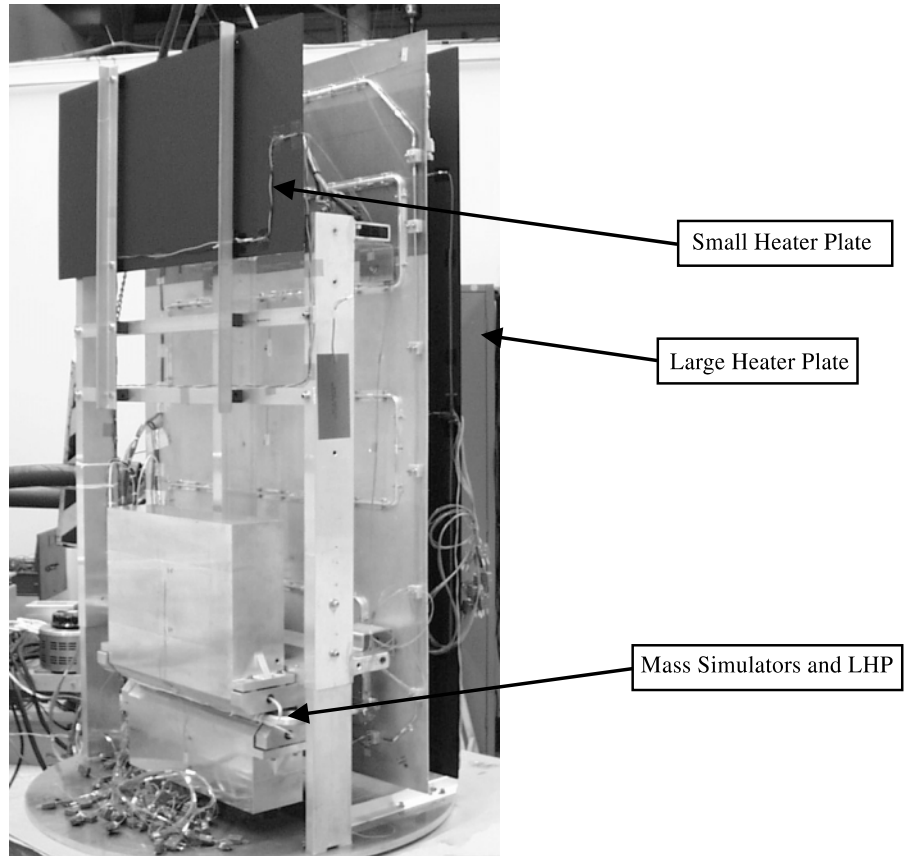


Figure 7. Heater Plates.

The heater plate setpoints were determined in test with the LHP operating in a fixed conductance mode. The setpoint was adjusted until the LHP radiator was operating at the same temperature as predicted in flight for hot case, cold case and survival case. Table 1 shows the heater plate setpoint used in the DM LHP test.

2.4 Test Plan

A wide variety of tests were conducted focussing on determining the control heater power, performing numerous startups, power cycling, and steady state tests. Table 2 shows most of the tests that were conducted. Emphasis was placed on measuring the control heater power tests and performing numerous startups.

Table 1. Setpoints for various

Thermal Case	Desired Average Radiator Temperature	Beta Angle and Yaw	Heat Sources	Setpoint - Large Heater Plate	Shroud Setpoint	Setpoint - Small Heater Plate
Hot/ss	-6 °C @ 120 W	Beta 33 Yaw 180	Avg Hot Solar, Avg Hot earth,	-18 °C - Reflux -24 °C - Adverse	-100 °C	-18 °C - Reflux -24 °C - Adverse
Cold/ss	-35 °C @100 W	Beta 90 Yaw 90	Cold Earth	-67 °C	-170 °C	-75 °C
Survival	-100 °C @ 0 W	Survival Mode	-100 °C on Radiator	-100 °C	-170 °C	-100 °C

Table 2. Thermal Vacuum Testing

Startup Heater (W)	Test	Power Cycle (W)	Orientation	Setpoint	Thermal Case
Establish Liquid - Vapor Line coupling (measure control Heater Power) Start with 8 liq-vap blocks					
20	Start-up	5 - 120W	Reflux	None-6.5 °C	Hot/ss
	Steady State	120 W	Reflux	6.5 °C	Hot/ss
Increase Liq-Vapor coupling blocks to 10					
	Steady State	120 W	Reflux	14 °C	Hot/ss
	Steady State	100 W	Reflux	14 °C	Hot/ss
	Steady State	120 W	Reflux	14 °C	Cold/ss
	Steady State	100 W	Reflux	14 °C	Cold/ss
	Steady State	100 W	Reflux	6.5 °C	Cold/ss
Start-up and Hot Case Transient Tests					
20	Start-up	5	Reflux	None	Survival
Transport Capability - Power Down					
	Steady State	100-200-300-400-15-0	Reflux	14 °C	Cold/ss
Long Term quasi-steady state					
	Transient/ Quasi-steady state	120	Reflux	0 °C	Hot/ss to Cold/ss
	Start-up	120	Adverse	None	Cold/ss
Flip the Test Setup-Repeat the tests from Reflux					
20	Start-up	5 - 120W	Adverse	None-6.5 °C	Hot/ss
	Steady State	120 W	Adverse	6.5 °C	Hot/ss
If the blocks have not been adjusted than following the tests					
	Steady State	120 W	Adverse	14 °C	Hot/ss
	Steady State	100 W	Adverse	Cold Case	Cold/ss
Start-up and Hot Case Transient Tests					
20	Start-up	5	Adverse	None	Survival
	Transient	120	Adverse	6.5 °C	Hot/tr
Transport Capability - Power Down					
	Steady State	100-200-250-300-100-50-0	Adverse	Cold Case	Cold/ss
Long term Steady State and quasi-steady state					
20	Long Term Steady State	15	Adverse	Cold	Cold/ss
20	Transient/ Quasi-steady state	120	Adverse	0 °C	Hot/ss to Cold
15	Start-up	5	Adverse	None	Survival

2.5 Thermocouple Diagram

Figure 8 shows the thermocouple diagram used for DM LHP. Note the LHP evaporator, starter heater, compensation chamber and liquid vapor coupling blocks. The circles in the lower right corner are the radial positions of the compensation chamber. The condenser and heater plates are shown in the upper right corner.

Figure 8. TC diagram.

3.0 STARTUP TESTS

LHP startups are characterized by the initiation of vaporized working fluid exiting the evaporator through the vapor line; and through the liquid line, cold liquid returning into the evaporator from the condenser. This is indicated during testing typically by a rapid rise in the vapor line temperature and drop in the liquid line temperature. Examining Figure 9 below, the startup was preceded by several cycles of the CC survival heater (from 6:50 to 8:08). At 8:09, 20 W is applied to the starter heater and 5 W is applied to the laser simulator. TC 1 is a TC right next to the starter heater. When the starter heater is turned on, TC 1 rapidly rises to be the warmest TC. The average evaporator and the compensation chamber then track TC 1. At 19:30, TC7 (the vapor line) rapidly rises and measures about the same temperature as the CC and the average evaporator indicating that vapor has boiled off from the evaporator and is now travelling into the vapor line enroute to the condenser. Fluid circulation, and therefore startup, was further evidenced by a rapid drop in the liquid line temperature to same temperature as the condenser.

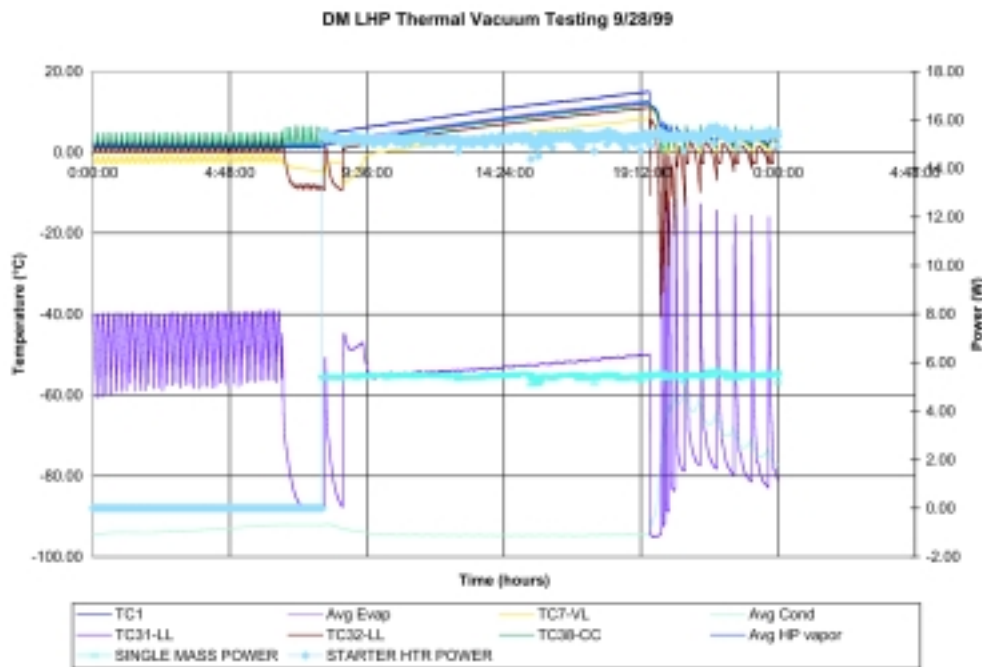


Figure 9. Typical startup.

All 17 startups are summarized in Table 3. Various initial conditions were explored. Startups were conducted in both the adverse and reflux orientations. The average condenser temperature was varied from -30 to -105 °C. The starter heater power was varied from 0 W to 30 W. In the last set of start-up profiles, the final startup was repeated with nearly identical conditions five (5) times to examine the repeatability of the startup tests.

A total of 17 startups were conducted. The overwhelming conclusions that can be drawn are —

- Startups take a long time (hours in most cases even when the evaporator is hot).
- Startups tend to occur in the range from 5 °C to 20 °C on the evaporator.
- All successful startups required a starter heater. Effects of various parameters on the start-up are elaborated on in the following sections.

Table 3. DM LHP Startup Matrix

Date	Orient Reflux/ Adverse	Start #	Single Mass Htr (W)	Starter Htr (W)	Initial Avg Evap (°C)	Initial CC temp (°C)	Initial Avg Condenser (°C)	Max Evap (TC1) °C	Avg Max Evap (°C)	Max CC temp (°C)	Heater Plate Setting	Time required for Startup	Comments
8/23	R	1	4.3	20-30	22	2.1	-60.	28.	25.	22.4	Surv	1:14	Condenser dropping
8/24	R	2	117.	19.7	-4.2	1.3	-30.	22.1	19.7	17.5	Surv	2:11	Condenser dropping
9/1	R	3	5.2	19.9	3.0	4.0	-34.	9.0	6.5	3.7	Hot	1:35	CC preheated
9/7	R	4	5.3	19.5	0.9	1.5	-34.	22.2	19.7	18.7	Hot	14:10	CC Cycling
9/9	R	5	5.3	19.7	-1.2	1.3	-94.	18.2	15.8	14.6	Surv	11:30	CC Cycling
9/12	R	6	5.4	20.4	0.5	1.0	-105.	17.5	15.0	13.8	Surv	9:30	CC Cycling
9/17	A	7	5.4	19.7	20.8	23.3	-70.	26.5	23.6	21.3	Cold	1:00	CC preheated, Condenser dropping
9/18	A	8	5.3	20.1	1.7	2.0	-89.	14.9	12.2	10.8	Surv	7:50	CC Cycling
9/19	A	9	5.5	20.2	-2.8	2.0	-95.	19.6	16.9	15.3	Surv	15:16	CC Cycling
9/20	A	10*	100	0	1.0	2.0	-70.	31.8	31.3	31.4	Cold	Did not Start	Did not Start
9/23	A	11	5.7	20.0	2.8	13.6	-73.4	17.9	15.	14.3	Cold	6:00	CC preheated to 14°C
9/23	A	12	5.7	20.1	9.9	14.1	-40.	Data was lost	Data was lost	Data was lost	Hot	Data was lost	LHP Started, but startup point was lost
9/26	A	13	5.5	15.4	2.1	3.4	-93.	18.2	15.9	14.6	Surv	16:15	CC Cycling
9/28	A	14	5.4	15.3	1.5	3.0	-95.	14.9	12.8	12.0	Surv	11:19	CC Cycling
10/4	A	15	5.6	15.3	0.8	2.5	-95.	20.4	18.2	16.8	Surv	20:54	CC Cycling
10/5	A	16	5.5	15.1	0.0	2.0	-94.	19.3	17.0	15.6	Surv	17:40	CC Cycling
10/6	A	17	5.4	15.1	-3.0	3.0	-94.	21.5	19.2	17.7	Surv	26:12	CC Cycling

*This test was ended before startup because the evaporator had reached the system design limit of 30°C

3.1 Effect of Initial Condenser Temperature

Examining the data in Table 3, very few trends can be predicted based on condenser temperature. This is clear when examining startups 3 and 4 in the hot case condenser temperature. Startup 3 had one of the quickest startups with one of the lowest maximum evaporator temperatures of any of the cases. However, Startup 4 was one of the slowest and had the highest maximum evaporator temperature. This “random” trend is also seen with colder sinks. Startup 17 and Startup 14 were identical condition startups with very different maximum evaporator temperatures. Startup is independent of condenser temperature, possibly due to the relatively small size of the condenser.

3.2 Effect of Initial Evaporator Temperature

Startups were performed at various initial evaporator temperatures from -4 to 21 °C. The GLAS system design requires the LHP to start prior to the evaporator reaching 30 °C. The LHP tended to start faster (require less time to start) the warmer the LHP evaporator was. That is clearly seen in Startup 7 where the initial evaporator temperature was 21 °C and the LHP started 1 hour later. This might not seem particularly fast, but the average startup required 12 1/3 hours. Conversely, Startup 17 had an initial evaporator temperature of -3 °C and the startup required 26 1/4 hours.

But startup time is less of a concern than maximum evaporator temperature reached during startup. In general, the evaporator rose at least 3 °C from its initial temperature, but typically much more if the evaporator was “cold.” This means that the initial temperature prior to startup must be sufficiently below 30 °C to prevent exceeding the system requirement. When all of the maximum evaporator temperatures are compared for all of the startups, as long as the evaporator temperature was below 15 °C initially, the maximum average temperature the evaporator would reach before startup was below 20 °C during all DM LHP startup test.

3.3 Effect of Single Laser Mass Simulator Power

The single laser mass simulator is a 15 Kg thermal mass attached to the LHP via a heat pipe. The power applied to the mass is dissipated through sensibly heating the mass and through being conducted to the evaporator. During startup tests, most (if not all) of the power applied to the laser simulator was required to sensibly heat the mass to “keep up” with the increasing evaporator temperature. The evaporator increased in temperature typically due to a starter heater, not through conduction from the laser simulator.

Most of the startup tests were conducted with 5 W on the laser simulator (based on the flight baseline design). In Startup 2, 120 W was applied to the laser simulator and it resulted in one of the hottest startups (20 °C). Larger amounts of power on the laser simulator tend to increase the rate that the system warms up, but do not cause the startup to occur at a cooler evaporator temperature. This makes sense because in addition to requiring a warm evaporator temperature to start the LHP, there is a factor of waiting a period of time until the CC temperature is sufficiently higher than the evaporator temperature and the fluid properties offer a possibility of startup. Startup is a random event based on the onset of nucleation boiling. Though the potential for LHP startup is a function of evaporator temperature, it is also a function of time. As mentioned in Section 3.2, the average startup required 12-1/3 hours and the shortest startup took about 1 hour. None of these startups were instantaneous. Therefore, increasing the amount of laser simulator power only tends to heat up the system faster, not start the LHP at a cooler temperature. There is no GLAS system requirement for the maximum allowable time for a startup.

It was attempted to start the LHP with laser simulator power alone, Startup 10, (which will be summarized in the next section.) The LHP did not startup below the maximum system temperature of 30 °C and the test was aborted. It was not felt that the LHP was near to starting either. The need for the starter heater to be activated for a startup is discussed in the next section.

3.4 Startup Heater Power Sensitivity (0 W, 15 W, 20 W)

One of the things unique to propylene is the ease at which it initiates nucleation boiling. This is because the latent heat and liquid surface tension are both much lower. This is both a help and a hindrance to LHP startups. The ease at which propylene boils will help the formation of bubbles in the vapor grooves (a necessary component in startup). But it also easily bubbles on the ID of the wick (part of the compensation chamber). This means that a propylene LHP always has a high thermal coupling between the evaporator and the compensation chamber during startup. In order to start the LHP, a superheat (and hence pressure difference) is required between the evaporator and compensation chamber to initiate the circulation. Superheat is the temperature difference between the localized vapor within the evaporator and the saturation temperature in the compensation

chamber. When heat is applied uniformly to the evaporator (such as through the laser mass simulator heat pipe), very little superheat is produced. But when a high heat flux starter heater is added to one end of the evaporator, a localized hot spot is produced which produces a much higher superheat.

The greatest superheat was possible when the starter heater was used (because of the heating in the most desirable area that is least coupled to the compensation chamber). DM LHP was tested both with and without a starter heater. Startup 10 was the startup without a starter heater, but with 100 W on the single laser simulator. After 2 hours and 20 minutes, the amount of superheat produced by applying power only on the laser simulator was only 0.4 °C. The startup was terminated because the evaporator had exceeded the system design limit. Examining Table 3, the average superheat at startup was 4 °C, an order of magnitude larger. It is possible at some greater temperature the LHP would have started, but it appears unlikely that it was imminent even when the laser simulator was 34 °C.

The effect of starter heater power was examined by varying between 15 W and 20 W of starter heater power, see Table 4. This was done on nine tests with 20 W and five tests with 15 W. Table 4 lists two different average maximum evaporator temperatures. The maximum average temperature is the average of all the maximum temperatures reached in each startup. TC1 was the thermocouple right next to the starter heater and therefore the warmest one on the evaporator. The other listed evaporator temperature is the maximum overall evaporator temperature (which is an average of all the evaporator TC's), averaged over all of the startups.

The fact that the 15 W starter heater tests on average started the LHP 1.5 °C warmer than the 20 W starter heater tests is a very interesting result. In fact, if Startup 3 is thrown out of the 20 W average, this difference completely goes away (and the standard deviation drops for the 20 W case). Throwing out Test 3 makes some sense because it was such an unusually quick startup, maybe as a result of not completely liquid filling the vapor grooves (which makes the startup more difficult). The fact that the averages are the same could be explained when looking at how the average startup time increases for the 15 W case substantially. One should be careful not to read too much into the increased startup times for 15 W, because all of the 15 W cases started from 0 °C. Not all startup cases started as cold as 0 °C in the 20 W cases. However, the startup times for the 15 W cases should be approximately 25 percent longer than the 20 W cases. This roughly matches the measured warmup rate for the system (with approximately 48 Kg of mass and 5 additional Watts on the single laser simulator) as 0.94 °C/hour when the 15 W starter heater is used and 1.26 °C/hour for the 20 W. Even the decrease in superheat for the 15 W seems to have a small negative effect on the maximum temperature reached during startup (which is the most important system concern). The standard deviation variation disappears when startup 3 is thrown out of the 20 W cases as stated above. From all of the startups, the 2 σ maximum predict of the evaporator temperature would be 24 °C.

0 W Startups would not be successful without a startup heater because the compensation chamber tends to track the average evaporator temperature (as shown in Startup 10). When heat is being applied via the heat pipe from the laser simulator, most of the energy in the laser simulator is going to heat up the system thermal mass and very little superheat is produced. By applying power to the startup heater, a small portion of the evaporator is superheated above the CC (which is what startup requires). It is not clear from the testing what the minimum startup power could be, but it is less than 15 W. The minimum flight system startup power (16.8 W) would be when the ICESat spacecraft bus is at 26 V.

Table 4. Startups vs. Starter Heater Power

Startup Tests	Avg of Max TC 1 Temps	Std Dev of Max TC 1 Temps	Avg of Max Overall Evap Temps	Std Dev of Max Overall Evap Temps	Time for Startup (hours)	Std Dev of Time for Startup	Avg Superheat	Std Dev of Avg Superheat
All with Starter Heater (T0<20 °C)	18.1 °C	3.6 °C	15.7 °C	3.7 °C	12:20	7:07	4.0 °C	0.7 °C
20 W Starter Heater Only	17.7 °C	4.3 °C	15.1 °C	4.3 °C	8:30	5:06	4.2 °C	0.7 °C
15 W Starter Heater Only	18.9 °C	2.5 °C	16.6 °C	2.5 °C	18:28	5:31	3.5 °C	0.4 °C

3.5 Reflux vs. Adverse Effects

Maximum evaporator startup temperatures and the duration of time for the startup appear to be independent of gravity orientation (reflux or adverse mode). The difficulty in assessing this parameter is the wide range of startup temperatures that have occurred in each orientation and the lack of testing in comparable preconditions and startup power applied. However, the warmest startup with 20 W applied to the starter heater and 5 W to the laser simulator occurred in the reflux mode. During Startup 4 the average evaporator temperature only reached 16.9 °C under the same conditions. This comparison was not adequate to establish any clear conclusions.

3.6 Repeatability of Startup Test

Examining Table 3, Startups 13 through 17 were all performed with the same conditions: 15 W on the starter heater and 5 W on the single laser simulator. On all other tests that had 20 W on the starter heater and 5 W on the single laser simulator, the sink conditions were varied and the initial evaporator temperature was varied. The similarity in all startup tests lies in that before all the tests, the compensation chamber was preheated above the evaporator. Table 4 lists statistics on the maximum evaporator temperature, superheat and duration of the startup. As was stated in Section 3.4, comparing the average maximum startup temperature and standard deviation between Startups 13 through 17 and all other similar startups, Startups 13-17 basically had the same standard deviation and same maximum startup temperature as the other similar startups. This means that the startup is basically independent of sink conditions (as long as the sink is initially below the evaporator temperature), initial evaporator temperature (as long as it is below 14° C), and relative time between startups (as long as the compensation chamber is preheated). It is essentially based on the random nature of superheat required for the onset of nucleate boiling at startup.

4.0 CONTROL HEATER POWER TESTS

Control heater power refers to the power provided to the active control heaters on the compensation chamber to maintain the LHP at a desired operational point. Measurement of the control heater power was a nontrivial exercise due to the tight bandwidth on/off controller. From Test 8 onward (see Table 5), the actual measured value was improved, and validated by an electronic duty cycle measurement device and strip chart. This increase in measurement accuracy was achieved by modifying the on/off controller to provide a sharper on/off voltage curve by using a thermister filter. The flight controller has a $\pm 0.1^\circ\text{C}$ control setpoint tolerance which resulted in numerous short on/off cycles which to be measured properly required a square voltage curve. The discussion in this section will mainly be based on Tests 8 onward, because of initial inaccuracies of the control power measurement.

The control heater used on the compensation chamber was a 20 W heater for most of the tests. In some of the tests, the control heater was adjusted to 10 W, which is the flight heater sizing. This was done to demonstrate that 10 W was sufficient to meet the flight requirements. The maximum steady state control heater power number was 2.9 W when 10 blocks were installed in a cold case with 120 W applied at the 14° C CC setpoint. The largest recorded transient control heater power was 4.6 Watts just after power was step changed from 100 W to 200 W.

The coupling blocks between the liquid and vapor lines serve the purpose of using the latent heat of the vapor line to warm the liquid return line temperature. Warming the liquid return line temperature decreases the control heater power requirement. The effectiveness of the coupling blocks is really based on the temperature difference between the liquid return line temperature and the saturation temperature. In Section 4.8 it will be shown that each coupling block has a fixed conductance coupling between the liquid and vapor lines. That means the energy transferred from the vapor line to the liquid line is simply a function of the temperature difference. If very little subcooling is available from the condenser, very little energy will be taken away from the liquid line and vice versa. So the coupling blocks have a large effect in a cold case and a small effect in a hot case.

Overall the control heater power tests were very positive. Table 5 lists the control heater power tests and the recorded control heater power.

Table 5. DM LHP Control Power Test Matrix 2.0

Tests #	# of coupling blocks	Single Mass Power (W)	Orientation	CC Setpoint (°C)	Thermal Case	Control Heater size (W)	Power Req't (W)	TC31	TC32	TC32 - TC 31	Date	W/ or W/o thermometer filter
1	8	120	Reflux	6.5	Hot/SS	20	3.2	-23	-4.3	19.	9/1	W/o
2	8	30	Reflux	6.5	Hot/SS	20	1.9	-32.1	5.6	38.	9/1	W/o
3	10	120	Reflux	6.5	Hot/SS	20	2.5	-23.	-2.7	20.	9/8	W/o
4	10	100	Reflux	14.	Cold/SS	20	3.1	-68.	2.0	70.	9/8	W/o
5	10	120	Reflux	14.	Cold/SS	20	3.6	-60.	0.3	60.	9/8	W/o
6	10	120	Reflux	14.	Cold/SS	11	3.7	-60.	0.3	60.	9/8	W/o
7	10	120	Reflux	14.	Hot/SS	20	3.0	-28.1	2.4	30.	9/10	W/o
8	10	100	Reflux	14.	Hot/SS	20	2.0	-33.	3.	36.	9/10	W/
9	10	100	Reflux	14.	Cold/SS	20	2.6	-66.1	1.0	67.	9/10	W/
10	10	120	Reflux	14.	Cold/SS	20	2.9	-60.	-0.5	60.	9/11	W/
11	10	120	Reflux	6.5	Cold/SS	20	2.8	-59	-8.	51.	9/11	W/
12	10	120	Reflux	6.5	Hot/SS	20	1.9	-20.	-3.	17.	9/13	W/
13	10	120	Reflux	14.	Hot/SS	20	2.4	-27.	3.4	30.	9/14	W/
14	10	100	Adverse	14.	Cold/SS	20	2.7	-51.	1.	52.	9/17	W/
15	10	120	Adverse	14.	Hot/SS**	20	1.8	-15.	4.5	20.	9/17	W/
16	10	120	Adverse	6.5	Hot/SS**	20	1.0	-8.	2.4	10.	9/17	W/
17	10	120	Adverse	6.5	Hot/SS	20	1.5	-18.	-1.	17.	9/21	W/
18	10	120	Adverse	14	Hot/SS	20	2.1	-22.	4.8	27.	9/21	W/

* Heater Power appears stable within 0.1 W

** Sink conditions in Adverse are different from Reflux. These early tests did not have the correct sink.

*** All of these tests were performed W/O a thermostat filter, and therefore the Power requirement was over-measured.

NOTE: TC31 is at the Condenser Exit of the liquid line, TC32 is after the coupling blocks right before the CC on the liquid line.

4.1 Control Heater Power Energy Balance

One of the most remarkable outcomes of testing the DM LHP was the low required control heater power. Prior to the testing of DM LHP, thermal models had predicted much larger control heater powers. This discrepancy is due to an assumption based on previous ammonia test data. Current modeling techniques for ammonia LHPs assume that the entire subcooling amount (or mass flow rate x liquid specific heat of the working fluid x temperature difference between the saturation temperature and the returning liquid temperature) is dumped into the compensation chamber. The subcooling amount or sensible cooling of the between the returning subcooled liquid and the saturation conditions in the compensation chamber. The subcooling amount or sensible cooling of the liquid return line in all of the tests are shown in yellow in Table 6. But the real measured control heater power is much smaller and is shown in red.

After observing this disparity and knowing that the liquid conductivity of propylene is only 40 percent of the liquid conductivity of ammonia, it was decided to lower the infinite coupling from the ammonia models to a coupling that fit the data and had physical significance. The calculated power based on this coupling is shown in green. The coupling assumes 0.19 W/K between the returning subcooled liquid and the saturation conditions in the compensation chamber.

The physical significance of this coupling is based on the assumption that the conduction between the liquid return line and the compensation chamber is dominated by the film coefficient of the returning liquid line. The DM LHP, like most LHPs, has a bayonet tube that enters the compensation chamber from the far end and passes down the centerline to empty the returning liquid at very opposite end of the evaporator. Flow through this bayonet tube is always laminar (even at 250 W), so assuming the film coefficient for a constant temperature boundary yields a constant Nusselt number of 3.66. The 0.19 W/K coupling, which roughly matches the data corresponds to a 6" coupling length in the compensation chamber. Physically the compensation chamber cylinder is 5.2" long and the transition tube is 1.7".

See Table 6 for the actual control heater power as compared to the calculated $\dot{m} \cdot c_p \cdot \Delta T$ formula and the 0.19 W/K coupling. It appears that this heater power equation is only related to the subcooled liquid temperature entering the compensation chamber, not to the orientation of the LHP.

To complete the energy balance, the remainder of subcooling (the difference between $\dot{m} \cdot c_p \cdot \Delta T$ and the actual applied control heater power) flows down the bayonet tube and exits at the opposite end of the evaporator. This liquid is then pulled into the wick and heated to saturation prior to vaporizing at the OD of the wick. Thus, the control heater requirement is substantially less than originally estimated, since the control heater does not have to "preheat" all of the returning sub-cooled liquid. This will result in a slightly lower mass flow rate when control heater power is used for the same power than when it is not used.

4.2 Temperature Stability

Temperature stability of the single laser simulator mass was very stable through most of the testing. Figure 10 shows temperatures on the single laser simulator after a setpoint change. The temperature requires 2.5 hours to stabilize and then it is stable within ± 0.1 °C for another 5 hours. As you can see from the plot, there is a lot of noise in the thermocouple. The temperature fluctuations that are shown in Figure 2 are a result of approaching the 'T' type thermocouple's precision limit of ± 0.1 °C. The GLAS system requirement is ± 0.3 °C.

4.3 Sink Condition Effect

The colder the liquid exiting the condenser as compared to the CC temperature, the greater amount of heater power required, see Figure 11. The control heater power appears basically linear, despite the coupling block's effect. Flight temperature differences could be as high as 80 °C in a cold orbit.

4.4 Sensitivity to Setpoint

Control heater power increases as the CC setpoint increases. This is the same thing as increasing the delta T between the compensation chamber and the condenser the amount the CC setpoint increases. It also happens to make the radiator panel operate more efficiently, lowering the condenser outlet temperature, compounding the delta T increase.

Table 6. Calculation of Control Heat Power

Test #	# of coupling	Single Mass Power (W)	Orientation	CC Setpoint (°C)	Thermal Case	Re	C (Liq Return to CC) W/K	Power Req'd (W)	Q calc'd from 6" line HAdT	Q cal'd mdot*cp*dT	TC31	TC32	TCCC -TC32	Date	W/ or W/o thermometer filter
1	8	122	Reflux	7.9	Hot/SS	1103	0.19	3.2	2.35	10.36	-23	-4.3	12.2	1-Sep	W/o
2	8	30	Reflux	6.5	Hot/SS	270	0.19	1.9			-32.1	5.6	0.9	1-Sep	W/o
3	10	120	Reflux	6.5	Hot/SS	1078	0.19	2.5			-23	-2.7	9.2	8-Sep	W/o
4	10	100	Reflux	14	Cold/SS	930	0.19	3.1			-68	2	12	8-Sep	W/o
5	10	120	Reflux	14	Cold/SS	1116	0.19	3.6			-60	0.3	13.7	8-Sep	W/o
6	10	120	Reflux	14	Cold/SS	1116	0.19	3.7			-60	0.3	13.7	8-Sep	W/o
7	10	120	Reflux	14	Hot/SS	1116	0.19	3			-28.1	2.4	11.6	10-Sep	W/o
8	10	101	Reflux	14.6	Hot/SS	942	0.19	2	2.24	8.48	-33	3	11.6	10-Sep	W/
9	10	101	Reflux	14.3	Cold/SS	940	0.19	2.6	2.56	9.71	-66.1	1	13.3	10-Sep	W/
10	10	121	Reflux	14.6	Cold/SS	1128	0.19	2.9	2.91	13.28	-60	-0.5	15.1	11-Sep	W/
11	10	121	Reflux	7.3	Cold/SS	1091	0.19	2.8	2.95	12.73	-59	-8	15.3	11-Sep	W/
12	10	124	Reflux	7.2	Hot/SS	1117	0.19	1.9	1.97	8.66	-20	-3	10.2	13-Sep	W/
13	10	123	Reflux	15	Hot/SS	1149	0.19	2.4	2.24	10.38	-27	3.4	11.6	14-Sep	W/
14	10	101	Adverse	14.6	Cold/SS	942	0.19	2.7	2.58	9.61	-51	1.2	13.4	17-Sep	W/
15	10	119	Adverse	14.6	Hot/SS**	1110	0.19	1.8	1.95	8.50	-15	4.5	10.1	17-Sep	W/
16	10	120	Adverse	6.9	Hot/SS**	1080	0.19	1	0.87	3.43	-8	2.4	4.5	17-Sep	W/
17	10	119	Adverse	6.9	Hot/SS	1071	0.19	1.5	1.52	6.20	-18	-1	7.9	21-Sep	W/
18	10	123	Adverse	14	Hot/SS	1144	0.19	2.1	1.77	7.95	-22	4.8	9.2	21-Sep	W/
19	10	205	Reflux	16	Survival	1925	0.19	3.2	3.0	23.9	-22.5	0.25	15.8	14-Sep	W/
20	10	201	Adverse	14.4	Survival	2536	0.19	1.81	1.8	13.5	-6.1	5.3	9.2	21-Sep	W/

**Sink conditions in Adverse are different from Reflux. These early tests did not have the correct sink.

NOTE: TC31 is at the Condenser Exit of the liquid line, TC32 is after the coupling blocks right before the CC on the liquid line.

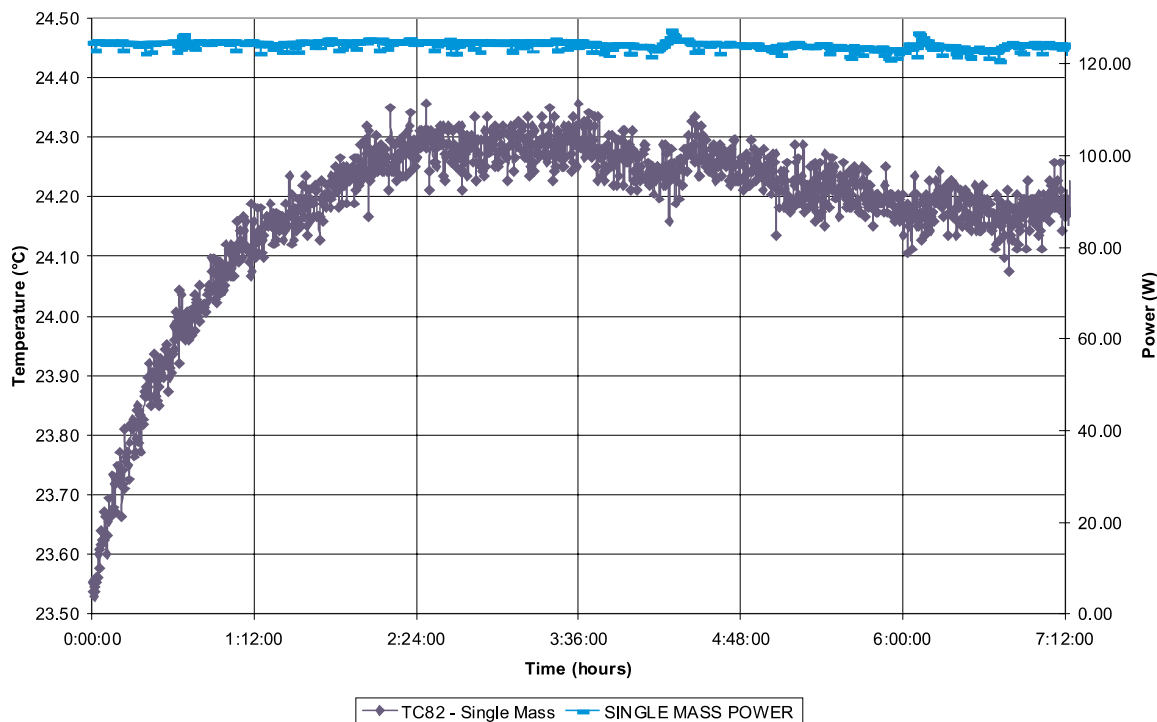


Figure 10. Temperature stability at the laser mass simulator.

The radiator panel operates more efficiently because the two phase fluid area (active area) in the condenser is at the saturation temperature (roughly CC setpoint temperature). Then when the CC setpoint is raised, the active area becomes shorter. This makes sense because the ability of a radiator to radiate energy is proportional to the difference between the fourth power of the radiator temperature minus the fourth power of the sink temperature. The required active area is therefore inversely proportional to this fourth power temperature difference for a fixed mass simulator power. When the active area is reduced, the returning liquid becomes increasingly subcooled. Notice this difference when Test 13 and 12 are compared in Table 6. In Test 13, the CC setpoint was increased 7.8 °C and this resulted in the condenser exit temperature dropping 7 °C. With a 15 °C additional temperature difference, using Figure 11, we should expect an additional 0.7 W of control heater power. The actual test data from Tests 12 and 13 show a 0.5 W addition, which is reasonably close.

When the setpoint is changed, settling time is required before the mass simulators become stable in temperature again. Figure 10 shows the settling time required for the mass simulators following such a setpoint change. During this test, after 2.5 hours the mass simulators were stable. In flight, settling times following setpoint adjustments also will be on the order of a few hours, although it was within ± 0.5 °C in less than 1 hour.

4.5 Sensitivity to a Changing CC Setpoint

Care must be taken to increase the CC setpoint slowly. If the transition is too fast, the LHP vapor grooves can become liquid filled shutting down the LHP. This occurs if the CC temperature exceeds the evaporator temperature and will require an additional startup with startup heater. The LHP is sensitive to this in operation, because power is only applied to the large thermal mass. If the setpoint of the LHP is increased rapidly the CC temperature will rise above the mass (because of the thermal inertia of the mass) and the heater power applied to the single mass simulator goes completely into sensible heat of the mass simulator. The heat flow can even be reversed such that heat flows from the evaporator to the laser mass simulator. In such a scenario, the CC becomes the heat source and the mass simulator, the heat sink. The evaporator temperature would then drop below the CC temperature flooding the vapor grooves. The vapor groove flooding is due to the compensation chamber temperature rising above the evaporator temperature and flooding the rest of the LHP as stated above. If the starter heater is activated, the startup heater can locally superheat a portion of the vapor grooves and prevent the LHP grooves from being flooded. The startup heaters ability to prevent the flooding of the vapor grooves was shown to be very stable through

many tests where, the CC survival thermostat provided thermal control for the LHP. In such tests, when the thermostat closed, the compensation chamber temperature rose 5 °C within 30 seconds. If the CC setpoint must be changed swiftly, the starter heater must be activated.

During testing of the LHP without the starter heater activated, the transition rate was examined with 100 W applied to the mass simulator. With 100 W on the LHP, 0.6 °C/5 minutes was an acceptable upward transition (did not shut off the LHP), see Section 8.0. The higher the applied heat to the mass simulator, the faster the allowable transition.

If a faster rate is chosen and the CC floods the liquid grooves in the evaporator, the LHP then must have the starter heater activated and another long startup process initiated. Lowering the setpoint is not of concern except that it can cause rapid cooldown of the components. Any change to the setpoint will require a stabilization time on the order of hours before all components in the heat pipe network reach equilibrium again.

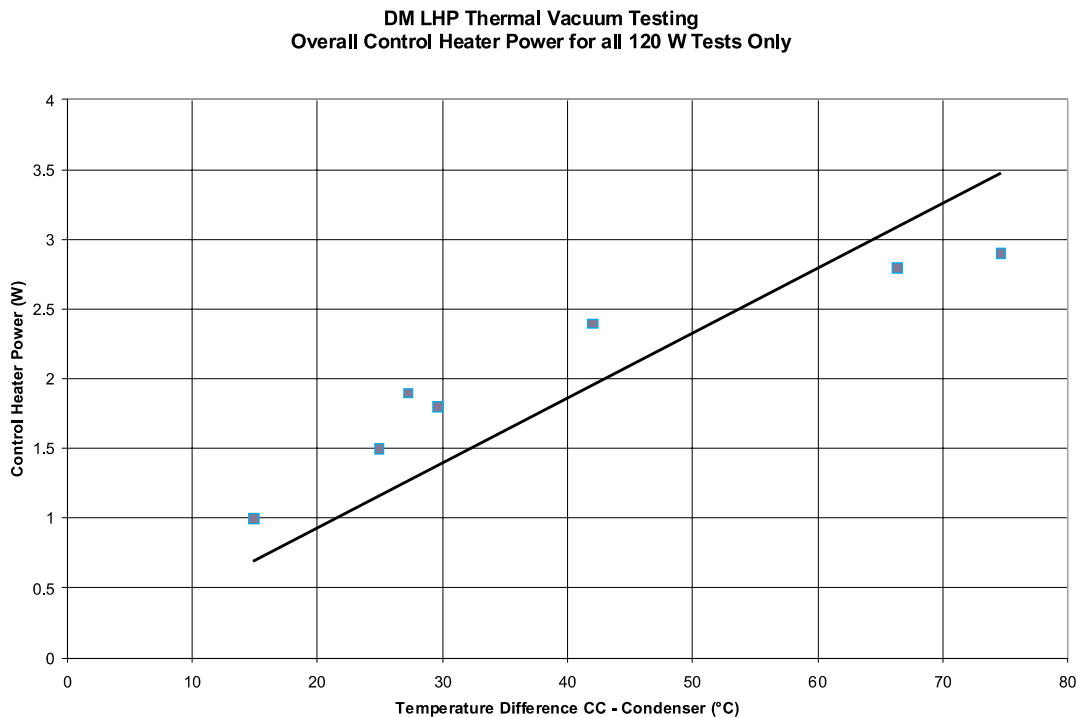


Figure 11. Control Heater Power vs. Delta T between CC and Condenser Exit.

4.6 Transient Sink Effects (with Fixed Conductance Mode)

Figure 12 shows a transient test where the sink was deliberately transiently changed to vary the LHP from variable to fixed conductance in a flight-like period. The test procedure for the transient test was to allow the heater plates to cool to -40 °C and then heat them to 0 °C so that the LHP reached fixed conductance mode in about 1/2 hour. The heater plates were maintained at 0 °C for about 15 minutes until the LHP was in fixed conductance mode for at least 15 minutes and then the heater plates were set again to -40 °C. After this the LHP re-entered variable conductance and slowly cooled. The heater power on the heater plates was calculated to transition the LHP from the steady state at -40 °C to fixed conductance in a 30 minute period.

The purpose of this sink transient was to evaluate the operation of the LHP when it switched between fixed and variable conductance and to evaluate the point of maximum transience possible in flight. Maximum transience was seen during the LHP cooling with approximately a cooldown rate of 3.4 °C/hour (with the test radiator of lower thermal mass than the flight). This occurs right after the LHP comes out of fixed conductance mode.

Control heater power during sink transience was somewhat an unknown. This is one of the first tests which evaluated this quantity and verified that it did not exceed system limitations. The control heater power requirement, because of the rapid cooling, was gladly not a problem. This can be explained because the control heater power is directly related to the temperature difference between the CC and the condenser exit temperature. The control heater power creeps up slowly when the sink is cooled. During temperature transience, the overall (orbit average) control heater power is fairly low since a large portion of the cycle is spent in fixed conductance mode when the control heater power is zero. There is no concern of short-term large peaks of control heater power due to sink transience because the peaks do not approach the higher cold case requirement.

4.7 Adverse vs Reflux

Examining Table 6, three tests were conducted in both reflux and adverse orientations for comparison. Tabel 7 compares the two tests in each respective orientation.

The model presented in Section 4.1 assumes that the liquid core has a weak thermal coupling with the compensation chamber. The comparison in Table 7 seems to back up this assumption. The control heater power shown does not vary greatly between the adverse and reflux orientations. Where in Test 12 and 13, the control heater power is greater than Test 17 and 18, the discrepancy can be explained due to the different temperature of the returning liquid from the condenser. Table 7 shows that the liquid exiting the condenser (TC 31) is colder in the reflux orientation. Because of the test setup, it was impossible to achieve identical sink conditions in both orientations.

The three comparison test results show that there is not effect of orientation on control heater power. This is a surprising finding. Most current LHP models calculate a heat leak across the primary wick based on pressure losses through the LHP between the CC and the Vapor grooves see Diagram 1. The temperature difference across the wick is then the required saturation temperature difference required to make the required saturation pressure loss as the fluid flows through the loop. The conductance through the wick is assumed to be basically constant. Because adverse elevation tests have a larger pressure loss, the current models calculate a higher heat leak through the wick beacuse the temperature difference increased. This should result in a lower control heater power measurement in adverse orientation versus reflux. Since tyhis effect is not seen in Table 7, the assumption that both sides of the wick are a t saturation conditions must be flawed. This was partially why the subcooled liquid core model ws presented in Section 4.1. In the model presented in this test report, we no longer calculate the heat leak through the wick (it is difficult to calculate due to a variance in liquid temperatures in the liquid core.) But we calculate the “subcooling leak” from the liquid return line to the compensation chamber by assuming it is a fixed conductance. The heat leak through the wick is then only the sensible heat of the returning liquid minus the subcooling leak into the compensation chamber from the liquid return line.

Table 7. Compare Control Heater Power vs. LHP Orientation

Reflux Orientation					Adverse Orientation				
Test #	Power Required (W)	TC31	TC32	Tcc-TC32	Test #	Power Required (W)	TC31	TC32	Tcc-TC32
9	2.6	-66.	1.	13.	14	2.7	-51.	1.	13.
12	1.9	-20.	-3.	10.	17	1.5	-18.	-1.	8.
13	2.4	-27.	3.	12.	18	2.1	-22.	5.	9.

4.8 Number of Block Couplings

The LHP was tested with two different numbers of 1" long liquid line to vapor line coupling blocks. The control heater power requirement for the 8 blocks Test No. 1 as compared to the 10 blocks Test No. 3 could not be assessed definitively because the tests were conducted before the controller thermistor filter was added (see Section 4.0) and therefore the control heat power estimations were overly high. With the high estimation, the 8 block originally tested required 3.2 W of heater power in the hot case, compared to the 10 block where the heater power requirement dropped to 1.9 W. The increase in coupling blocks is also seen in comparing the temperature difference between the CC and TC32 (a TC on the Liquid line after the coupling blocks). Both of these tests were under the same sink and orientation conditions. The liquid exit to the condenser (TC31) is at the same temperature before the blocks. But further up the liquid line, with 10 blocks, the liquid line is warmed to -2.7 °C. With 8 blocks the temperature is only warmed to -4.3 °C.

The critical number in calculating the control heater power is the difference between the CC and TC32 as mentioned above. This delta T is 12.2 °C for 10 blocks, and with 8 blocks it is 9.2 °C. The ratio 3.2 W /2.5 W also is basically equal to 12.2 °C/ 9.2 °C. From the calculation and explanation in Section 4.1, the control heater power is proportional to the temperature difference between the returning liquid (TC32) and the CC temperature. The TC32 temperature is dependent on the TC31 (condenser exit temperature) and the coupling between the vapor line and liquid line. The overall coupling varies with the number of blocks; the coupling per block is basically constant.

In Section 4.3 it was observed that the control heater power was also proportional to the temperature of the liquid exiting the condenser (TC31). The liquid/vapor coupling blocks thermal coupling between the liquid line and the vapor temperature (compensation chamber temperature), therefore must have a proportionality constant, which is proportional to the amount of blocks. Table 8 lists the proportionality constant per coupling block. Statistics are also included for comparing the 14 tests. One standard deviation is +11 percent of the average coupling. This is not the best correlation, but over a wide variety of tests and the quasi-steady state nature of the liquid return line temperature, this is not a bad variation.

Using the average value from Table 8, the test value was compared to an analytical value. The conductance between the liquid line to the vapor line is dominated by the forced convection film coefficient on the ID of the liquid line. The Reynold's number on the liquid line is ~950 for 100 W, 1100 for 120 W and 1925 for 205 W. This meant that the mean flow rate for the above tests were laminar. But the actual test data shows a Nusselt number 2.7 times the laminar, fixed-temperature boundary, and fully developed flow Nusselt number. More careful analysis of the flow pattern shows that 18" of coupling is required before the thermal boundary layer is fully developed. Therefore, the developing thermal boundary layer should be a Nusselt number that is 1.455 times the developed thermal boundary layer per curve fit by Hausen. But the test data shows a Nusselt number 85 percent higher than even this value. Therefore there must be something that is enhancing the Nusselt number. Michael Nikitkin of DCI theorizes that NCG bubbles flowing through the LHP enhance the local turbulence increasing the film coefficient in the coupling block area. Dan Butler of GSFC explains the enhanced film coefficient as possibly due to the natural pressure and flow oscillations within the LHP, just as seen in the CPL during normal operation that increases the effective Reynolds number within the liquid line.

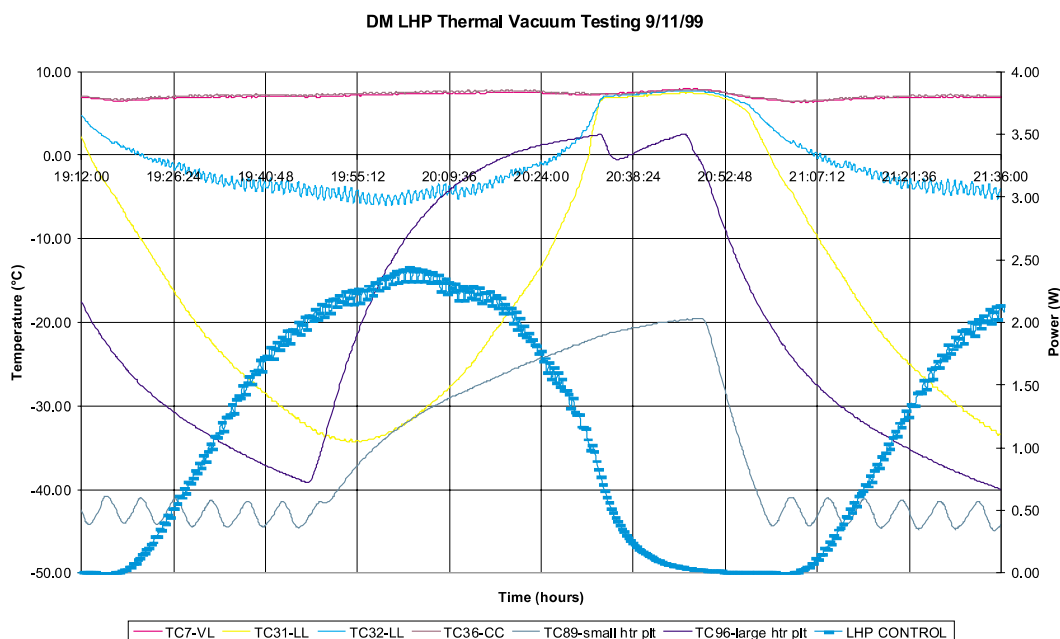


Figure 12. Control Heater Power Transient.

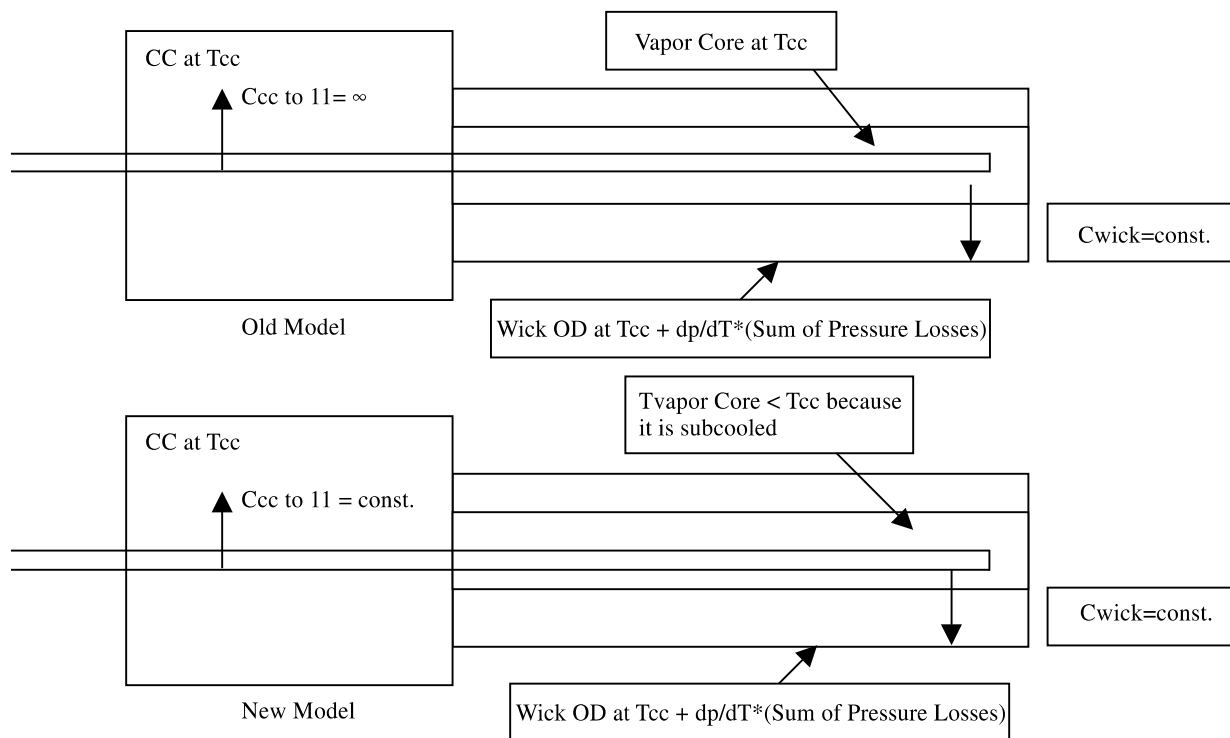


Diagram 1

4.9 Effect vs. Laser Simulator Power

Adding power to the laser simulator (which in turn increases the power to the LHP and mass flow rate) has been typically understood to increase the control heater power. However for the reasons described in Section 4.1, the conductance between the liquid return line and the compensation chamber is fixed independent of flow rate (which is proportional to laser simulator power and LHP power). This is true as long as there is sufficient flow rate such that the liquid return line continues to dump subcooled liquid into the liquid core. The corresponding power related to this minimum sufficient flow rate was not evaluated. Since all of the testing did have sufficient power, the minimum power where the coupling to the CC is independent of power must be below 100 W. It is anticipated, at lower flow rates, the control heater power would be a function of the flow rate. Correspondingly at very high power (above 210 W), the liquid return line would become highly turbulent and the control power might again become a function of applied power. But for the GLAS application where powers are between 100 and 210 W and control heater power is being utilized, the control heater power is independent of laser simulator power.

Control heater power tests were conducted with identical conditions with the laser simulator power varying from 100 to 120 W to examine this idea. From Table 6, Test No. 8 with 101 W and Test No. 13 with 123 W have 2 W and 2.4 W control heater power measurements respectively for the same ΔT (11.6 °C) between the liquid line (TC32) and the compensation chamber. This may seem to counter the above assertion that control heater power is independent of mass flow rate. But when Test No. 20 with 201 W (twice the mass flow rate) is compared having 1.8 W of measured control heater power for a 9.2 °C temperature difference between the liquid line and the compensation chamber, the independence of control heater power and mass flow rate is made clear. Tests 9 and 10 are also under the same conditions. For Test 9 with 101 W and a 13.3 °C temperature difference, 2.6 W are required. For Test 10 with 121 W and a 15.1 °C temperature difference, 2.9 W are required.

The increase in heater power from Test 9 to Test 10 can solely be attributed to the greater temperature difference because $13.3/15.1 \text{ °C/°C} \sim 2.6/2.9 \text{ W/W}$.

5.0 LHP CONDUCTANCE/TRANSPORT

The evaporator conductance looks good: 24 W/K versus the 22 W/K requirement. The flight saddle will utilize Aluminum 6063 versus the DM LHP saddle Aluminum 6061 so even higher conductances are expected at flight. The condenser conductance also meets or exceeds specification. The evaporator conductance is measured by dividing the inputted power to the single thermal mass by the temperature difference between the heat pipe vapor and the LHP CC vapor temperature. The condenser conductance is measured by dividing the inputted power to the single thermal mass by the temperature difference

between the LHP CC vapor temperature and the average condenser temperature, as measured by thermocouples on the top of the condenser extrusion.

Overall transport was limited by the radiator and radiator sinks. In the worst case adverse orientation, the LHP and radiator operated with 250 W applied. In reflux the LHP operated at 300 W. No evaporator deprime effects were observed.

5.1 Evaporator Conductance

Table 9 lists the assumptions used in a SINDA model of the DM LHP evaporator. The results as compared to test data are shown in Figures 13 and 14.

The LHP convection coefficient used in this data correlation was derived from ammonia film coefficient data provided by DCI. DCI's advertised convective coefficient for ammonia LHPs is 25,555 W/m² K. During GLAS breadboard LHP testing with both ammonia and propylene as working fluids, it was discovered that propylene conductance was only 80 percent of ammonia's conductance. Therefore for this correlation, an 80 percent factor on DCI's original ammonia convective coefficient was used (20,444 W/ m² K). A lower convection coefficient of 10,000 W/ m² K was put into the model to evaluate the sensitivity of the model to the LHP film coefficient. But this film coefficient did not correlate with the test data at all. This indicates that a film coefficient around 20,000 W/ m² K is probably correct.

For the test configuration, two separate cases were run: a 205 W and 114 W case. Figures 13 and 14 show actual SINDA node temperatures, with accompanying thermocouple data from the DM test. The arrows show the actual test data, while the SINDA output temperatures are shown within the column and row data. The vapor node of the LHP was set to the same value for the test and for the SINDA Analysis. Very good agreement was made between test results and the SINDA model, thus giving confidence in predicting performance of the flight configuration.

5.2 Condenser Conductance

Condenser conductance was only examined in cases where the LHP was operating without control heater power. The condenser conductance is measured by dividing the inputted power to the single thermal mass by the temperature difference between the LHP CC vapor temperature and the average condenser temperature as measured by thermocouples on the top of the condenser extrusion (as stated above). The requirement from the flight LHP spec (GLAS-545-SPEC-005) is 57 W/K for the Laser LHP and 100. W/K for the component LHP. In Table 10, the first three tests represent the Laser LHP and the last three tests represent the component LHP. All DM LHP test met the condenser conductance requirements for the flight LHPs.

Condenser conductance tends to be lower for lower input powers. This occurs because the heat leak from evaporator to the compensation chamber is more significant at lower powers. When heat leaks from the evaporator to the compensation chamber at low power, the condenser becomes more liquid-blocked. This liquid blockage lowers the overall condenser conductance. The heat leak increases when the LHP is oriented in the adverse mode than in the reflux mode. The test with 70.6 W/K conductance for 120 W represents such a case. The sensitivity to the evaporator to CC heat leak decreases with power. The adverse orientation case with the 300 W is not as sensitive to the evaporator to CC heat leak.

The overall variation in condenser conductance is not surprising, because it becomes increasingly difficult to measure conductances this high. Flight conductances will be somewhere between the reflux orientation conductances and the adverse orientation conductances and exceeding the system requirements.

Table 8. Individual Test Block Couplings

Test #	C per block (W/K)
1	0.079
3	0.081
9	0.092
10	0.097
11	0.088
12	0.070
13	0.090
14	0.084
15	0.077
16	0.088
17	0.081
18	0.099
19	0.101
20	0.072
avg	0.086
std dev	0.010
std dev/avg	0.113

Table 9. Assumptions for DM LHP Evaporator Model

Assumption	High Power, DM	Low Power, DM
LHP material	Alum 6061	Alum 6061
LHP heat load (Watts/ft. length)	205	114
LHP temperature (°C)	16.2	-1.7
Interface material thermal conductivity (W/m K)	0.2 Apiezon L Grease	0.2 Apiezon L Grease
Interface material thickness (in).	0.00067 0.00067	
Heat pipe convection coefficient (W/m ² K)	11,360 @ Ø.318" fin tip	11,360 @ Ø.318" fin tip
LHP convection coefficient (W/m ² K)	20,444 @ wick OD	20,444 @ wick OD

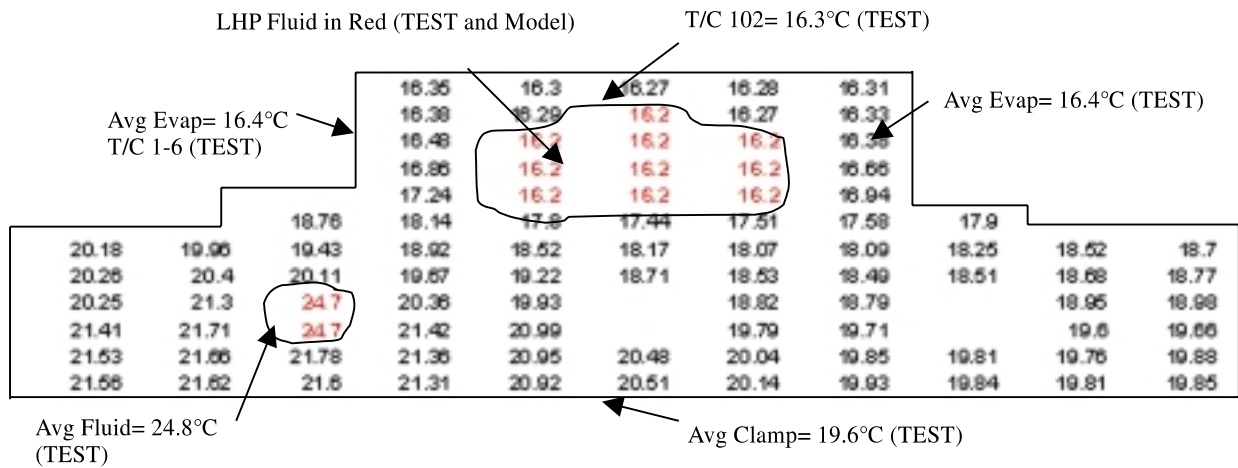


Figure 13. LHP DM 205 W temperatures compared to test data.

6.0 POWER TRANSIENTS

Power transients were not a major problem for DM LHP. The large thermal masses of the system prevent any instantaneous power changes at the laser simulators from rapidly effecting the power the LHP “sees.” This makes the operation of the LHP more reliable and stresses the secondary wick less. Power changes were made at DCI from 20 W to 210 W to 20 W. No adverse effects were noted.

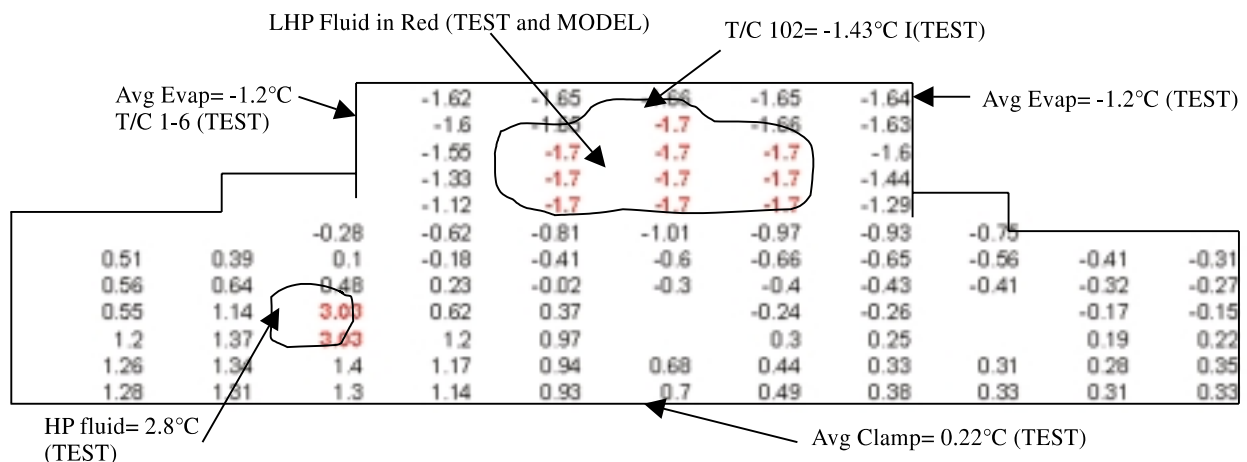


Figure 14. LHP DM 114 W temperatures compared to test data.

Table 10. Condenser Conductance

Single Mass Power (W)	Orientation	CC Setpoint (°C)	Thermal Case	TC31	TC32	TC32 -TC31	TCCC -TC32	Date	Avg Cond Temp (°C)	Cond Conductance W/K
120	Reflux	-2	Hot/SS	-2.1	-2.3	0.2	0.3	25-Aug	-2.8	150.0
100	Reflux	-31.4	Cold/SS	-31.7	-31.6	0.1	0.2	26-Aug	-32.2	125.0
120	Adverse	-0.9	Hot/SS	-9.8	-3.9	5.9	3	18-Sep	-2.6	70.6
248	Reflux	16.8	Survival	16	16.5	0.5	0.3	15-Sep	15	137.8
300	Reflux	27.3	Survival	24.5	26.7	2.2	0.6	15-Sep	25.7	187.5
257	Adverse	25.5	Survival	22.5	24.6	2.1	0.9	22-Sep	24.2	197.7

7.0 LOW POWER LONG TERM STEADY STATE TESTS

The only long term steady state with low power applied was conducted with the compensation chamber survival heater exerting the thermal control. Because of the wide bandwidth of the thermostat and rapid setpoint change, the LHP could only be operated with the starter heater activated. Figure 15 shows a test where 15 W was applied to the starter heater and 5.5 W was applied to the single mass simulator. The LHP operated flawlessly until the test was concluded.

The oscillations observed during this test are due to the compensation chamber being thermostatically temperature controlled by a survival heater. As is clear by observing the liquid line, the circulation of the LHP would stop while the compensation chamber temperature rose. The moment the thermostat opened, circulation continued again without requiring an additional startup. If the same test had been conducted without the starter heater, the LHP would require a startup with the starter heater (with a evaporator temperatures climbing to ~18° C) every time the thermostat would close and the circulation stop. This is due to the low thermal mass of the compensation chamber and high power survival heater (~20 W) as compared to the rest of the system which has a very high thermal mass to input power ratio.

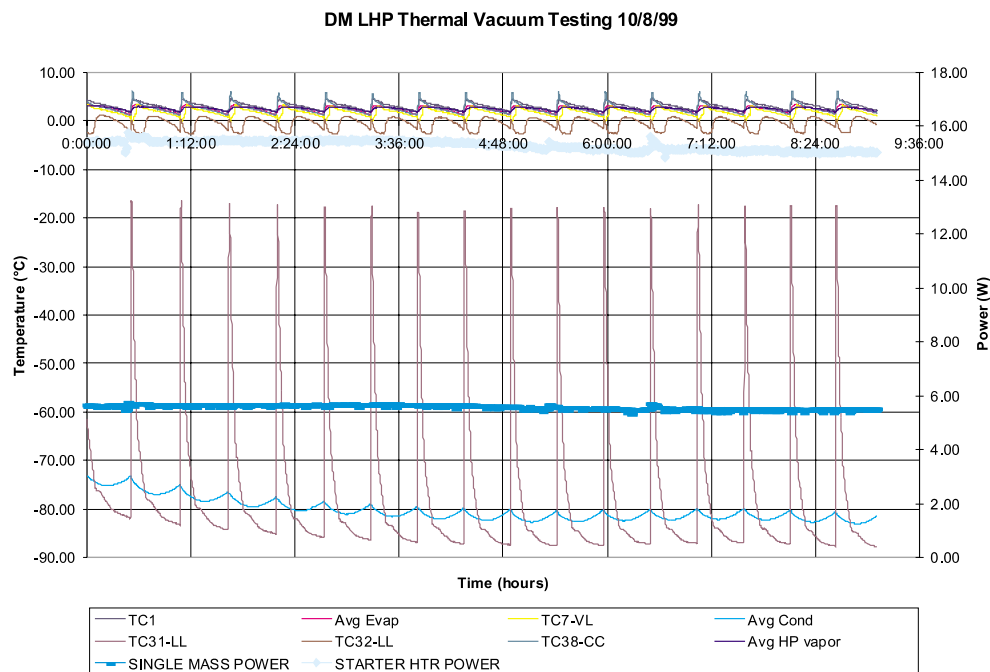


Figure 15 - Low power long term steady state.

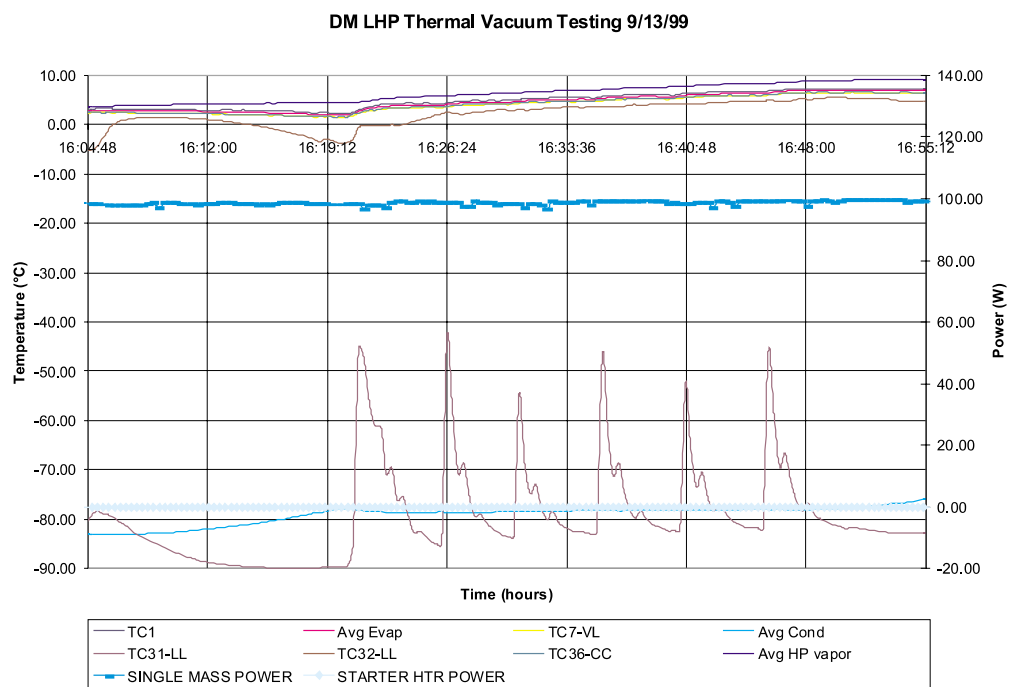


Figure 16. Increasing setpoint at a rate of 0.6° C/5 minutes.

8.0 PREVENTING THE CC FROM FLOODING THE EVAP

A test was conducted to demonstrate an acceptable CC setpoint increase rate. Figure 16 shows the CC setpoint carefully being increased in 0.6 °C increments every 5 minutes, while 100 W was applied to the LHP. This sensible heating of the system equates to 90 W of power. It has also been observed that if the starter heater is activated, there is no limit to CC setpoint change. This is because the starter heater ensures a portion of the vapor groove will stay vapor due to its high power to thermal mass ratio. Decreasing the CC setpoint is also not a problem, because then the sensible heat is dumped into the LHP.

In flight, all setpoint changes should be at a rate less than 0.6 °C/5 min if the starter heater is not turned on.

9.0 CONCLUSIONS

A total of 17 startups were conducted. Various initial conditions were explored. The overwhelming conclusions that can be drawn are: startups take a long time (hours in most cases even when the evaporator is hot), startups tend to occur in the range from 5 °C to 20 °C on the evaporator. All successful startups required a starter heater (15 - 20 W Dale Ohm Resistor), but all startups using the starter heater were successful.

The maximum steady state control heater power number was 2.9 W when 10 blocks were installed in a cold case with 120 W applied at the 14 °C CC setpoint. The largest recorded transient control heater power was 4.6 Watts just after power was step changed from 100 W to 200 W.

Care must be taken to always have the starter heater activated if the electronic thermal controller is disabled. Otherwise the on/off bandwidth of the CC startup heater will shut the LHP off every time it cycles. The LHP can only be re-turned on with the activation of the starter heater and waiting the required time for the LHP to start.

10.0 TV TEST RECOMMENDATIONS

The Flight LHPs will be similar to DM LHP but not identical. The following comments outline recommendations for an acceptance thermal vacuum test on the Flight LHPs:

- Verify multiple startups with the starter heater
- Measure the control heater power in the worst hot and cold cases and verify number of coupling blocks always maintain positive control heater power
- Verify allowable upward setpoint transition rates for flight, without shutting off the loop or activating the starter heater
- Mimic a flight transient case to verify sufficient margin that LHP stays in control always maintain positive control heater power
- Measure temperature of components during the flight transient to verify controllability of the LHP
- Measure system conductance

REPORT DOCUMENTATION PAGE			Form Approved OMB No. 0704-0188	
Public reporting burden for this collection of information is estimated to average 1 hour per response, including the time for reviewing instructions, searching existing data sources, gathering and maintaining the data needed, and completing and reviewing the collection of information. Send comments regarding this burden estimate or any other aspect of this collection of information, including suggestions for reducing this burden, to Washington Headquarters Services, Directorate for Information Operations and Reports, 1215 Jefferson Davis Highway, Suite 1204, Arlington, VA 22202-4302, and to the Office of Management and Budget, Paperwork Reduction Project (0704-0188), Washington, DC 20503.				
1. AGENCY USE ONLY (Leave blank)		2. REPORT DATE December 2000		3. REPORT TYPE AND DATES COVERED Technical Publication
4. TITLE AND SUBTITLE Geoscience Laser Altimeter System (GLAS) Final Test Report of DM LHP TV Testing			5. FUNDING NUMBERS 545.0	
6. AUTHOR(S) C. Baker				
7. PERFORMING ORGANIZATION NAME(S) AND ADDRESS (ES) Goddard Space Flight Center Greenbelt, Maryland 20771			8. PERFORMING ORGANIZATION REPORT NUMBER 2000-02554-0	
9. SPONSORING / MONITORING AGENCY NAME(S) AND ADDRESS (ES) National Aeronautics and Space Administration Washington, DC 20546-0001			10. SPONSORING / MONITORING AGENCY REPORT NUMBER TP—2000-209898	
11. SUPPLEMENTARY NOTES				
12a. DISTRIBUTION / AVAILABILITY STATEMENT Unclassified—Unlimited Subject Category: 18 Report available from the NASA Center for AeroSpace Information, 7121 Standard Drive, Hanover, MD 21076-1320. (301) 621-0390.			12b. DISTRIBUTION CODE	
13. ABSTRACT (Maximum 200 words) Two loop heat pipes (LHPs) are to be used for thermal control of the Geoscience Laser Altimeter System (GLAS), planned for flight in 2001. One LHP will be used to transport 100 W from a laser to the radiator, the other will transport 210W from electronic boxes to the radiator. In order to verify the LHP design for the GLAS application, an LHP Development Model has been fabricated, and ambient and thermal vacuum tested. Two aluminum blocks of 15 kg and 30 kg, respectively, were attached to the LHP to simulate the thermal masses connected to the heat sources. A 20 W starter heater was installed on the evaporator to aid the loop startup. A new concept to thermally couple the vapor and liquid line was also incorporated in the LHP design. Such a thermal coupling would reduce the power requirement on the compensation chamber in order to maintain the loop set point temperature. To avoid freezing of the liquid in the condenser during cold cases, propylene was selected as the working fluid. The LHP was tested under reflux mode and with adverse elevation. Tests conducted included start-up, power cycle, steady state and transient operation during hot and cold cases, and heater power requirements for the set point temperature control of the LHP. Test results showed very successful operation of the LHP under all conditions. The 20W starter heater proved necessary in order to start the loop when a large thermal mass was attached to the evaporator. The thermal coupling between the liquid line and the vapor line significantly reduced the heater power required for loop temperature control, which was less than 5 watts in all cases, including a cold radiator. The test also demonstrated successful operation with a propylene working fluid, with successful startups with condenser temperatures as low as 100°C. Furthermore, the test demonstrated accurate control of the loop operating temperature within +/- 0.2°C, and a successful shutdown of the loop during the survival mode of operation.				
14. SUBJECT TERMS Thermal Component, Two-Phase, Propylene, Thermal Control, GLAS, Loop Heat Pipes, LHP, Thermal Vacuum, heat pipe			15. NUMBER OF PAGES 27	
			16. PRICE CODE	
17. SECURITY CLASSIFICATION OF REPORT Unclassified	18. SECURITY CLASSIFICATION OF THIS PAGE Unclassified	19. SECURITY CLASSIFICATION OF ABSTRACT Unclassified	20. LIMITATION OF ABSTRACT UL	

